# A Variable-Impedance Prosthetic Socket for a Transtibial Amputee Designed from Magnetic Resonance Imaging Data

David Moinina Sengeh, MS, Hugh Herr, PhD

## ABSTRACT

This article evaluates the design of a variable impedance prosthetic (VIPr) socket for a transtibial amputee using computer-aided design and manufacturing (CAD/CAM) processes. Compliant features are seamlessly integrated into a three-dimensional printed socket to achieve lower interface peak pressures over bony protuberances by using biomechanical data acquired through surface scanning and magnetic resonance imaging techniques. An inverse linear mathematical transformation spatially maps quantitative measurements (bone tissue depth) of the human residual limb to the corresponding prosthetic socket impedance characteristics. The CAD/CAM VIPr socket is compared with a state-of-the-art prosthetic socket of similar internal geometry and shape designed by a prosthetist using conventional methods. An active bilateral transtibial male amputee of weight 70 kg walked on a force plate–embedded 5-m walkway at self-selected speeds while synchronized ground reaction forces, motion capture data, and socket-residual limb interface pressures were measured for the evaluated sockets. Contact interface pressure recorded (using Teksan F-Socket™ pressure sensors) during the stance phase of several completed gait cycles indicated a 15% and 17% reduction at toe-off and heelstrike, respectively, at the fibula head region while the subject used a VIPr socket in comparison with a conventional socket of similar internal shape. A corresponding 7% and 8% reduction in pressure was observed along the tibia. Similar trends of high-pressure reductions were observed during quiet single-leg standing with the VIPr socket in comparison with the conventional socket. These results underscore the possible benefits of spatially varying socket wall impedance based upon the soft tissue characteristics of the underlying residual limb anatomy. (*J Prosthet Orthot*. 2013;25:129–137.)

**KEY INDEXING TERMS:** variable impedance, compliant prosthesis, Polyjet Matrix 3D Printing, MRI, prosthetic socket, transtibial amputee

It is estimated that approximately 1.7 million Americans live with a limb loss, and that number is expected to double by the year 2050.[1] Discomfort in prosthetic sockets continues to be a critical challenge faced by both prosthetists and amputees. The quality and comfort of a prosthetic socket can determine the daily duration for which patients use their artificial limbs and also may prevent further pathological outcomes for amputees, especially soft tissue damage such as ulcers and blisters. Reproducible, comfortable prosthetic sockets, either passive or active, remain elusive, although there are complex robotic knees and ankle-foot prostheses.[2,3]

Presently, comfortable prosthetic socket production is mostly a craft activity, based primarily on the experience of the prosthetist. Even with advances in computer-aided design and computer-aided manufacturing (CAD/CAM), prosthetists often have to modify sockets using a nonquantitative craft process requiring substantial man-hours. Furthermore, prosthetists seldom integrate comprehensive quantitative anthropomorphic data and material properties into the design process or use CAD/CAM processes to fully design and manufacture the final socket for amputees.[4]

DAVID MOININA SENGEH, MS, is affiliated with Harvard University, and Massachusetts Institute of Technology, Cambridge, Massachusetts.

HUGH HERR, PhD, is affiliated with Millersville University, Pennsylvania; Massachusetts Institute of Technology, Cambridge, Massachusetts; and Harvard University, Cambridge, Massachusetts.

Funding source: Massachusetts Institute of Technology Media Lab Consortium.

Current affiliation of the authors: MIT Media Lab.



*Correspondence to: David Moinina Sengeh, Biomechatronics Group, MIT Media Lab, 75 Amherst Street, Cambridge, MA 02139; email:dsengeh@mit.edu*

## LITERATURE REVIEW

### CONVENTIONAL SOCKET DESIGN

State-of-the-art socket manufacturing has its limitations. To produce a socket, the prosthetist has to capture the three-dimensional (3D) shape of the residual limb by wrapping a cast around it while the residual limb is either loaded or unloaded, depending on the preference of the prosthetist. A positive mold of the residual limb is then acquired from the negative mold. The anatomical points of interest are identified on the positive mold and extra material is either added to relieve pressure at sensitive regions or removed to increase pressure at specific load-bearing locations.[5]

### COMPUTER-AIDED DESIGN AND COMPUTER-AIDED MANUFACTURING

Computer-aided design and manufacturing have been used to improve prosthetic sockets for many decades now, partly by

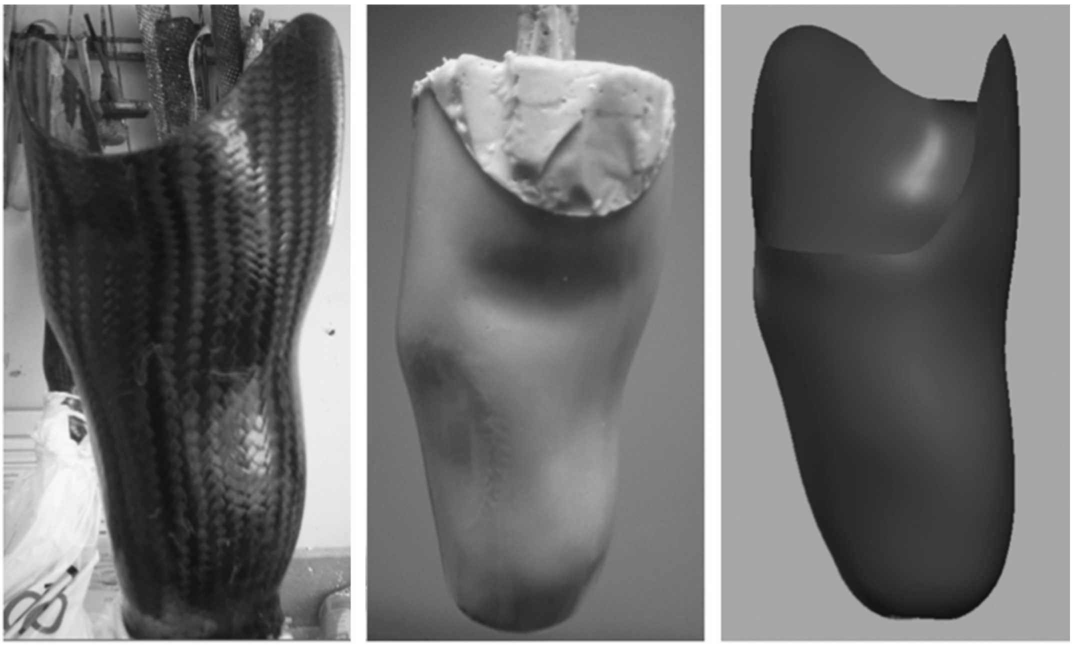

Figure 1. Left to right, conventional socket, male plug for the conventional socket, and an STL file exported from the scanning software trimmed to match the original cut lines of the socket.

changing the compliance of the prosthetic socket. Compliance in prosthetic sockets over anatomical landmarks reduces socket interface pressure, which is a major reason for sores, pain, and discomfort in sockets.[6–8] As both mechanical design and manufacturing technology have evolved in the medical field, so has the integration of CAD/CAM into prosthetic design. The surface shape of amputees' residual limbs is acquired by directly scanning the limb or a generated positive mold of the limb. Some CAD/CAM processes used in socket design and fabrication include computer numerical controlled milling of a positive mold, stereolithography, selective laser sintering, fused deposition modeling, laminated object manufacturing, and inkjet printing techniques for the fabrication of the final socket.[9–14] Compliance over bony protrusions, a means to relieving pressure, has been achieved by changing socket wall thickness[15] or by adding mechanical features to a single-material socket to increase its compliance.[6]

## ACQUISITION AND USE OF BIOMECHANICAL DATA IN COMPUTER-AIDED DESIGN AND MANUFACTURING SOCKET DESIGN

A variety of imaging processes have been explored for applications in socket design. Ultrasound has been used to capture the external surface shape and internal tissue distributions of a residual limb for use in socket design.[16–18] Magnetic resonance imaging (MRI) and computed tomography are other imaging tools that have been integrated into CAD/CAM socket design.[19–21] Even though advanced imaging tools are used to acquire the surface and internal tissue distribution of residual limbs, limited progress has been made toward a manufactured socket whose properties, including geometric shape and mechanical material properties, are quantitatively determined by the shape and biomechanical impedances of the underlying residual limb anatomy.

## SIGNIFICANCE OF STUDY AND HYPOTHESIS

This work presents a CAD/CAM approach to producing a seamless variable impedance prosthetic (VIPr) socket for transtibial amputees using quantitative biomechanical data from advanced surface scanning and MRI technology. Polyjet Matrix™ 3D printing technology is used to seamlessly integrate variable durometer materials into the socket design to achieve intrinsic spatial variations in socket wall impedance while maintaining structural integrity. The designed socket material properties are determined by the impedance of the residual limb as a means of achieving reduced socket–residual limb interface peak contact pressures for an amputee during dynamic walking and quiet standing activities. We hypothesize that an inversely proportional relationship between residual limb stiffness and the corresponding socket wall stiffness at each spatial location across the residual limb surface will lead to reduced contact pressures on bony protrusions during level-ground walking and quiet standing. As a preliminary evaluation of this hypothesis, a VIPr socket is designed, fabricated, and then compared with a conventional prosthetic socket designed by a prosthetist using standard best-of-practice methods. Although distinct in their wall impedance characteristics, the evaluated VIPr and conventional sockets have similar internal geometry and shape. In a preliminary clinical investigation, an active bilateral transtibial male amputee walks on a force plate–embedded 5-m walkway at self-selected speeds while synchronized ground reaction forces, motion capture data, and socket-residual limb interface pressures are measured for the evaluated sockets.

## METHODS

### INTERNAL SURFACE GEOMETRY CAPTURE

Because this study sought to understand the effects of spatially varying prosthetic wall impedances on socket interface pressures, the evaluated VIPr socket and conventional socket were fabricated to have identical internal geometry and shape. To capture the internal socket shape of the amputee's conventional socket, a positive mold of the participant's conventional socket was formed using alginate (Figure 1). No modifications were made to the internal socket shape before creating the positive mold. FastSCAN™, a system manufactured and supplied by Polhemus (Colchester, VT, USA), was used to capture the surface shape of the resulting positive mold. Images were exported from the FastSCAN software and converted to STL files, from which a CAD socket was designed. Three-dimensional surface images of the amputee's conventional prosthetic socket shape were imported into SolidWorks (Dassault Systèmes SolidWorks Corporation, Waltham, MA, USA). The STL mesh files were transformed into surfaces in SolidWorks. The proximal cut lines of the designed VIPr socket were similar to those used in the conventional socket (see Figure 1).

### MAPPING RESIDUAL LIMB STIFFNESS TO SOCKET STIFFNESS

#### *Estimation of residual limb stiffness*

Magnetic resonance imaging is a noninvasive imaging technique that relies on the magnetic properties of the nucleus in hydrogen atoms to spatially map the distribution of hydrogen atoms in a body segment. This project used MRI data of the residual limb of the amputee participant as a means of estimating and mapping body stiffness and anatomical landmarks directly to the VIPr prosthetic socket's wall stiffness. From the MRI data, one can approximate the stiffness of each location on the residual limb from the distances between the bone and the outside surface of the skin on each independent 2D magnetic resonance image. Although there are various image processing toolboxes and software, this project used the Mimics Innovation Suite® (v.13.0; Materialise, Leuven, Belgium) to segment and analyze the MRI data. The Mimics toolbox was used to calculate bone tissue depth at each anatomical location and to create an accurate 3D representation for the entire residual limb. Here, bone tissue depth

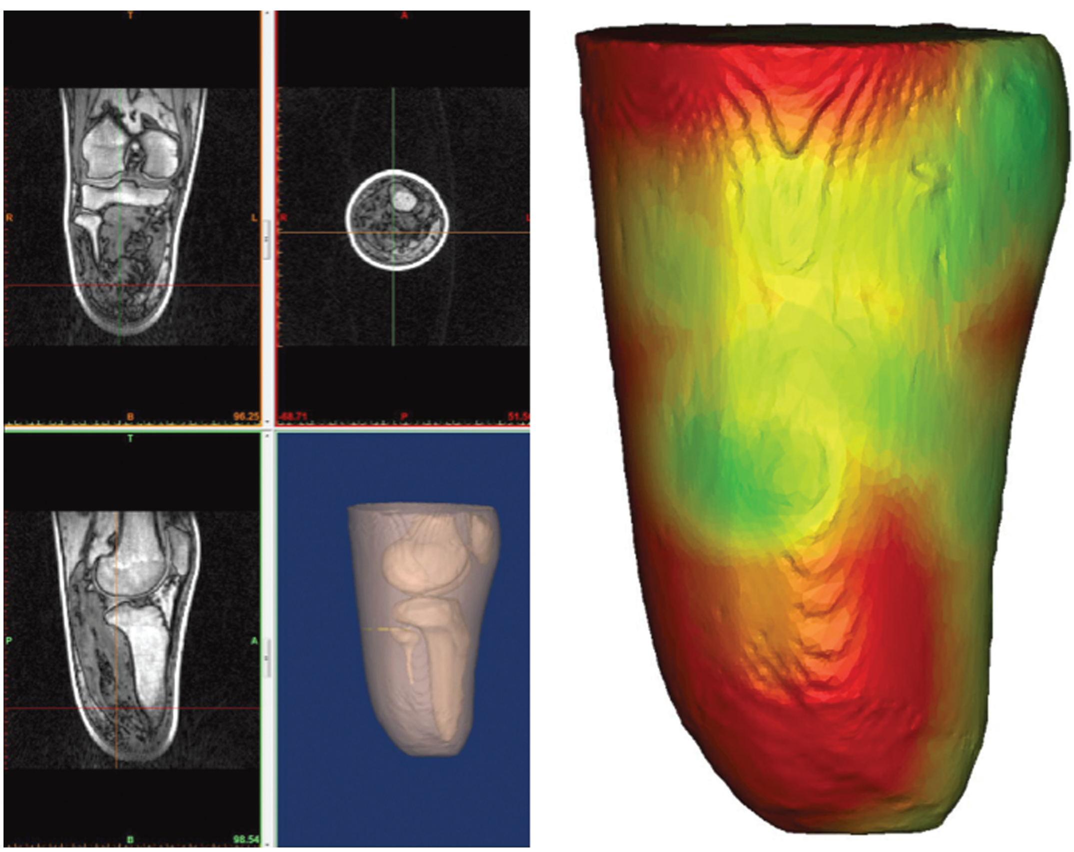

Figure 2. Left, four MRI views of the right residual limb of the amputee participant. Upper left, anterior view; upper right, lateral view; lower left, medial view; lower right, 3D rendering showing bones within the limb. Right, bone tissue depth representation is shown, where red denotes the maximum bone tissue depth and green denotes the minimum depth. The bone tissue depth range is as follows: green, 0–9 mm; and red, 20–50 mm. MRI, magnetic resonance imaging; 3D, three-dimensional.

**Figure 3.** Top row, three-dimensional (3D) computer-aided design of the variable impedance prosthetic socket, and the corresponding 3D printed socket is shown in the bottom row. Orientation for all images in both rows from left to right is anterior, lateral, medial, and posterior.

is defined as the orthogonal distance between the surface of the skin and the intersection of bone tissue when the body is not being compressed and is in a state of equilibrium.

In Figure 2, the left images represent four MRI views of the residual limb being analyzed, whereas the right image is a representation of the tissue depth measurement using the Mimics Innovation Suite. The green regions represent where the bones are closest to the skin, whereas red regions represent the regions that are furthest away from the surface of the skin.

### *Inverse linear map between bone tissue depth and socket material stiffness*

An inverse linear equation is used to map bone tissue depth to socket material stiffness properties. Regions where the body was stiffest interfaced with the most compliant material, whereas regions where the body was softest interfaced with the least compliant material. Using the Mimics software, a text file was generated with estimates of bone tissue depth at each location on the residual limb. The minimum depth was identified from the bone tissue depth dataset and was mapped to the minimum modulus of elasticity used for the 3D printing material, or 1.1 GPa. The maximum tissue depth, defined by the threshold value used to create the color map in Mimics, was 50 mm and was mapped to the maximum modulus of the 3D printed material, or 3 GPa.

The equation generated from the above values is as follows:

$$Y = 0.0382 \times X + 1.0882 \qquad (1)$$

(1)where $Y$ is the Young's Modulus of the printing material and $X$ is the bone tissue depth. Equation 1 represents an inverse relationship between socket material modulus and the

**Table 1.** Material properties used for FEA for the carbon fiber conventional socket and the two primary 3D printed materials used in the VIPr socket

| Property | VeroWhitePlus | Carbon fiber | TangoBlackPlus |
|---|---|---|---|
| Elastic modulus in X | $2 \times 10^9$ N/m$^2$ | $2 \times 10^{11}$ N/m$^2$ | $1.4 \times 10^9$ N/m$^2$ |
| Poisson's ration in XY | 0.394 | 0.25 | 0.394 |
| Tensile strength in X | $3 \times 10^7$ N/m$^2$ | $4 \times 10^9$ N/m$^2$ | $1 \times 10^6$ N/m$^2$ |
| Yield strength | $5 \times 10^7$ N/m$^2$ | $3 \times 10^8$ N/m$^2$ | $1 \times 10^6$ N/m$^2$ |

FEA, finite element analysis; VIPr, variable impedance prosthetic; 3D, three-dimensional.

impedance of the residual limb's soft tissue, approximated by bone tissue depth.

## THREE-DIMENSIONAL PRINTING OF THE VARIABLE IMPEDANCE SOCKET

From the different CAD environments, the completed socket design was exported or saved as STL file formats with the following properties: a deviation of 0.0005 in and a 5° angle to maximize the quality and detail of the design exported for printing. Because there were multiple materials with different properties in the design, each file corresponding to a different material type was saved as a unique file.

Objet Geometries Inc (Billerica, MA, USA) produces an advanced 3D printer that uses their PolyJet Matrix Technology. This technology enables two different material types to be simultaneously jetted in the production of the same model using the Connex™ printer with a build tray size of 500 mm × 400 mm × 200 mm. With a 16-μm, high-resolution print layer, high dots-per-inch in both X and Y resolution, and an easy-to-remove support material property, this technology was ideal for the development of multimaterial prosthetic socket prototypes.

In Figure 3, the designed CAD socket and the final 3D printed socket are shown. Truss structures were included as additional design features to enhance structural integrity to the socket by transmitting the high load from the stiff patella tendon region to the equally stiff distal posterior wall. The addition of the "truss" on the VIPr socket at the indicated locations did not affect the MRI-determined material stiffness at those locations. The material property of the truss was the same as the MRI-determined materials at the location where it connected to the socket, and that impedance was maximized or highly rigid. Thus, the socket impedance for a displacement perpendicular to the inner socket surface at each inner point was largely unaffected by the addition of the trusses.

The Objet™ Digital Materials that provided the most variability in material properties required by our design were a combination of VeroWhitePlus™ and TangoBlackPlus™. VeroWhitePlus has a modulus of elasticity ranging from 2 to 3 GPa and tensile strength ranging from 50 to 65 MPa. TangoBlackPlus has a tensile strength ranging from 0.8 to 1.5 MPa.

The 3D printed VIPr socket was postprocessed by a prosthetist while keeping the internal socket shape unchanged between VIPr and conventional sockets. A distal support block for the pyramid was designed such that any standard prosthetic pyramid could be attached to the bottom of the socket. A metal base was glued to the bottom of the socket with some Coyote Design Quick Adhesive CD4150. Multiple rolls of Techform Premium Casting Tape™ (Coyote Design & MFG, Boise, ID) of appropriate length were used in the anteroposterior and the mediolateral directions to enclose the metal base.

## FINITE ELEMENT ANALYSIS OF THE COMPUTER-AIDED DESIGN SOCKET

Even though this project combined multiple materials into one socket through 3D printing based on biomechanical information, the final VIPr socket had to be structurally sound to accommodate the dynamic walking activities of an amputee. It was assumed that all materials other than the stiffest material in the socket had negligible additional effects on the structural integrity of the socket and were thus removed from the part to be analyzed. The SolidWorks SimulationXpress™ package on the SolidWorks™ 3D CAD (Dassault Systèmes SolidWorks Corp, Waltham, MA) software was sufficient for the evaluation of the socket once it was reduced to a single material. Using a single material simplified the analysis and represented the worst-case scenario for structural integrity. Clearly, the overall factor of safety (FOS) would increase only if the softer materials within the socket wall were included in the analysis.

To estimate the FOS for the VIPr and conventional sockets, we conducted a finite element analysis (FEA) for the case of running, the most dynamic activity the amputee participant could undergo while using the socket interfaces. The properties of the socket materials used for this FEA are presented in Table 1. For this analysis, the pressure exerted on the inner socket wall by the residual limb was assumed to be uniformly distributed. Uniform pressure was computed as $P$ = (force/area). To calculate the area ($A$), a simplified circle was extracted from the sketch that forms a planar circumference around the fibula head and the proximal end of the tibia. The estimated diameter ($D$) was 0.0952 m. Thus, area ($A$) at that plane was estimated to be $(D/2)^2 = 7.1 \times 10^{-3}$ m$^2$.

The mass of the study participant was 70 kg, and thus, his weight was 686 N ($W = 70 \times 9.8$). To test for structural integrity, we used a force equal to 3 W (2058 N) as the maximum dynamically applied axial load applied to the socket during running. Thus, uniform pressure within the socket was estimated to be $P = 2058/(7.1 \times 10^{-3}) \approx 290$ kPa.

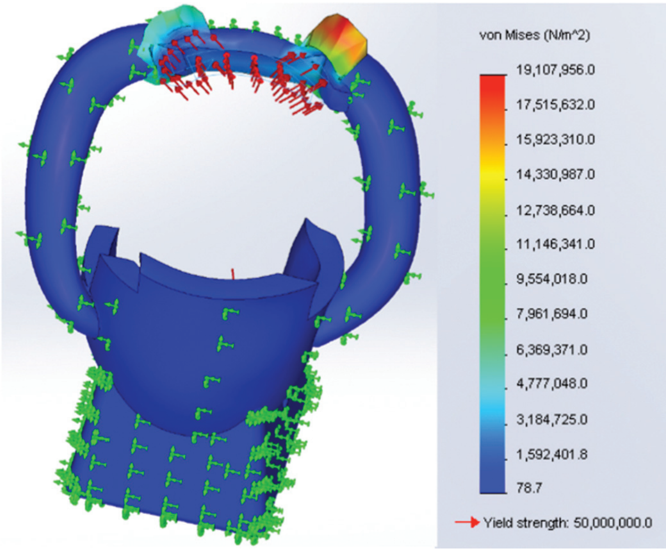


Figure 4. von Mises stress representations of a completely bound socket when walking toe-off forces are applied using material properties of VeroWhitePlus.

Near toe-off in running, a point force was assumed to act upon the patella tendon region to account for the additional torque experienced on the socket structure. This added force was approximated as $F = 3\ \mathrm{W} \times \cos(\Theta)$, where $\Theta$ is equal to the pitch angle of the residual limb's longitudinal axis from the horizontal. This estimated patellar force, $F$, is perpendicular to the longitudinal axis and was assumed equal to $F = 1.93$ kN when $\Theta = 20°$, assuming a vertical force equal to 3 W. For this estimate, the pitch angle of the lower leg at toe-off in running was taken from the literature.[22] Using the VeroWhitePlus material in the FEA, the FOS while running in the socket was estimated to be 2.01 (Figure 4).

As a comparison with this VeroWhitePlus material, using the same forces and conditions described earlier for a conventional carbon fiber socket material on the same CAD socket, the FOS increased to 11.96 during running at toe-off, a more than fivefold increase compared with the highest durometer 3D printed material used in this study. This result underscores the structural limitations of the 3D printed material used in this study compared with conventional prosthetic socket materials such as carbon composite. If the softer, lower-durometer 3D printed materials were assumed in the FOS estimate, the VIPr would not be structural. For example, when the TangoBlackPlus material was used in the same conditions described previously, the FOS was estimated to be 0.040 for running at toe-off.

## CLINICAL EVALUATION

The Committee on the Use of Humans as Experimental Subjects at Massachusetts Institute of Technology (MIT) approved the protocol used in this project. In the study, the VIPr socket was compared with a state-of-the-art carbon prosthetic socket of similar internal geometry and shape designed by a prosthetist using conventional methods. The properties of the two sockets evaluated in this study are summarized in Table 2. An active bilateral transtibial male amputee of weight 70 kg walked on a force plate–embedded 5-m walkway at self-selected speeds while synchronized force, motion capture data, and socket-residual limb interface pressures were measured for the evaluated sockets. Socket alignment was performed by a trained prosthetist and was similar for each prosthetic intervention evaluated. The subject walked using the VIPr socket for 30 minutes before data collection. Each socket was held firmly onto the residual limb during walking activities using a standard suspension sleeve. The same prosthetic components were used for each socket, including ankle-foot and foot cover components (Össur VSP® [Össur Americas, Foothill Ranch, CA] and cover) and prosthetic socket attachment hardware.

## INTERFACE PRESSURE MEASUREMENT

The interface pressures between the socket and the residual limb were evaluated with special attention to specific anatomical features including the tibia and fibula head regions. Pressure was measured using the F-Socket™ Pressure System provided by Tekscan, Inc (South Boston, MA, USA) at 100 Hz while the participant underwent single-leg standing. In addition, socket pressures were recorded as the participant walked 10 times at self-selected speed across a force plate–loaded walkway while motion capture data were recorded.

The pressure sensors were attached to the outside surface of the residual limb liner using double-sided tape to prevent displacement during tests (Figure 5). The flexibility, thickness, and other properties of the sensor are specifically optimized for measuring pressure in prosthetic sockets. The sensors were calibrated using Tekscan's default walk calibration, which uses body weight and a standard level-ground walking trial to

Table 2. Properties of evaluated sockets

| Property | Conventional socket | Variable-impedance three-dimensional printed socket |
|---|---|---|
| Mass, kg | 0.4811 | ≈1.4 |
| Internal geometry | Same | Same |
| External geometry | Different | Different |
| Material | Carbon fiber | Objet Digital Materials |
| Compliance | None | Yes |

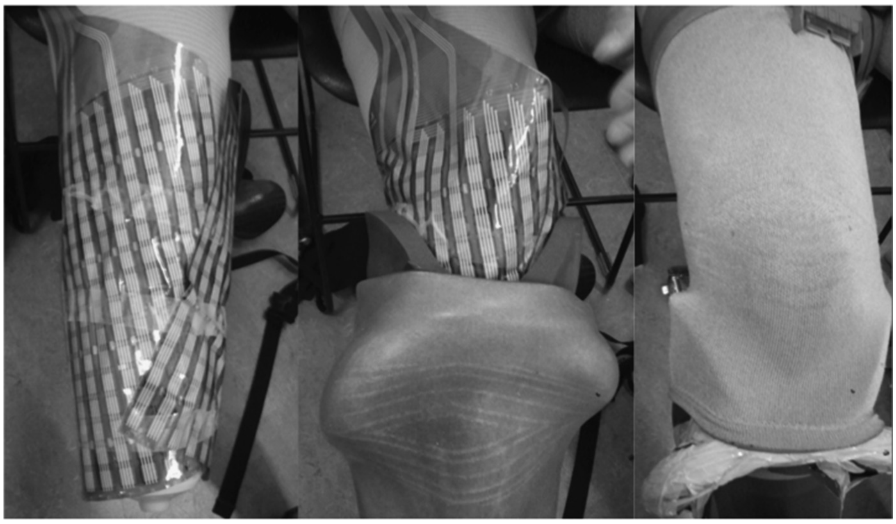

**Figure 5.** Pressure sensors are taped on to the liner to cover the entire residual limb (left). The limb is then inserted into the socket (center), and a sleeve is rolled over the limb for suspension (right).

calibrate all sensors. To remain consistent across trials, we applied the same walking calibration file to each recording.

We used the VICON 512 motion analysis system (Oxford Metrics, Oxford, United Kingdom) to track kinematics as the amputee walked at a self-selected speed across a walkway embedded with two force plates (Advanced Mechanical Technology Inc, Watertown, MA, USA). We placed 27 reflective markers mostly on the lower limb of the participant using the Helen Hayes maker set. The pressure readings from the sensors were synchronized to the motion capture recordings using a triggering signal (high to low voltage change) from the VICON system at the start and end of each trial. Force plate measurements were fed directly into the VICON system and automatically synchronized with marker trajectories. We determined heelstrike and toe-off using ground reaction forces, which allowed us to extract stance phase and the corresponding interface contact pressure values.

The sensors stayed in the same place during data collection for both the conventional socket and the VIPr socket. We made certain that the sensors were in the same location by pressing on specific cells on the residual limb during various stages of the experimentation. We ensured that the cells on the sensor over the fibula head, for example, were the same throughout the experiments. Where the sensors overlapped, we took readings from the sensor closest to the body. Before and after each trial, pressure readings were recorded for some locations, and these were later crosschecked to show that there was little to no location change during the experiments.

## RESULTS

Not surprisingly, the highest pressures recorded were during the stance phase of walking. During stance, two peaks were observed, as shown in Figures 6 and 7. The first peak occurred just after heelstrike at about 30% stance phase, whereas the second, higher peak occurred right before toe-off of the same leg at about 75% stance phase. During walking trials, the peak contact pressures recorded at the residual limb–socket interface were generally lower when the amputee participant used the VIPr socket compared with the conventional socket.

Specifically, while the participant walked at a preferred speed using the VIPr socket, we observed a 17% and 15% reduction in peak contact pressure on the fibula head region for the first and second peaks, respectively, in comparison with the conventional socket (Figure 6). A corresponding 8% and 7% reduction in contact pressure was observed along the tibia region (Figure 7). For these experiments, the preferred walking speeds of the participant were 0.84 and 0.72 m/s while using the VIPr and conventional socket, respectively. At the fibula head and tibia regions during single-leg standing, use of the VIPr socket also produced lower interface contact pressures of 13% and 21%, respectively (Figures 8 and 9).

## CONCLUSION AND FUTURE WORK

Using conventional socket technology, nearly all amputees experience residual limb discomfort due in part to excessive pressures over anatomical points. In this investigation with a single study participant, we showed that the contact pressures over the fibula and tibia anatomical landmarks were decreased in a VIPr socket during preferred speed walking and single-leg standing in comparison with a uniformly rigid conventional socket. Furthermore, we observed a 16% increase in the self-selected walking speed of the participant while using a VIPr socket.

In this study, the VIPr socket was nearly three times heavier than the conventional carbon socket. The present weight of the VIPr socket is caused by the poor mechanical properties of its 3D printed materials and the resulting large socket-wall thicknesses necessary to achieve structural integrity. The FOS of the

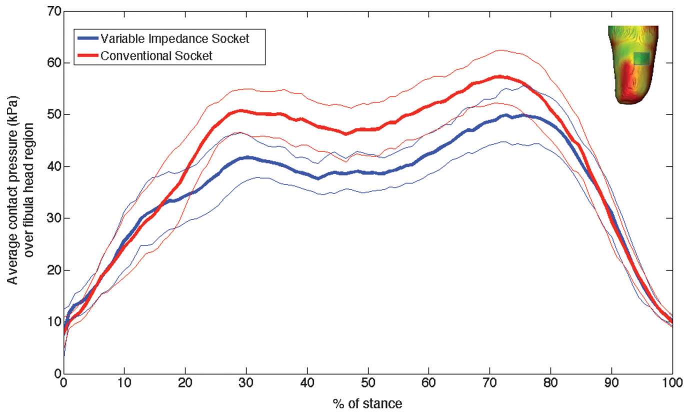


Figure 6. Contact pressures for the variable impedance prosthetic socket and the conventional socket for the same fibula head region (shown as the darkened box on the image of the residual limb) are plotted versus percentage stance period. Shown are mean pressure data ± 1 SD for $n$ = 10 walking gait cycles measured at a preferred gait speed.

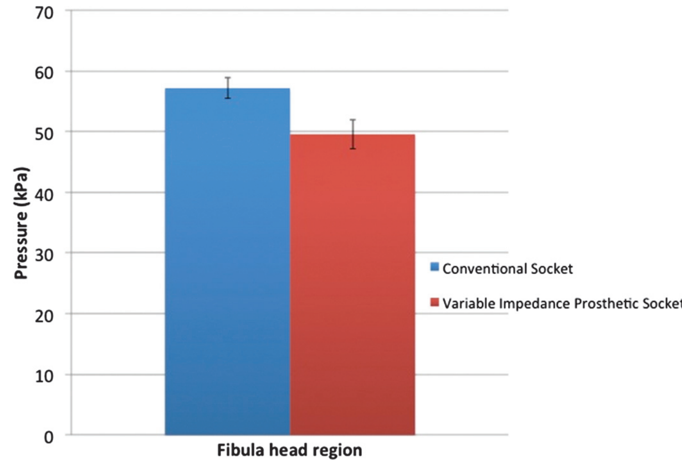


Figure 8. Mean contact pressures ± 1 SD for the two socket interventions measured over the same fibula head region during single-leg standing for 4 seconds at 100 Hz.

lighter conventional carbon socket far exceeded that of the heavier 3D printed VIPr socket. If the library of 3D printed materials grows to contain materials of higher Young's Modulus and higher tensile strengths, the weight of a 3D printed VIPr design and the thickness of its walls could be further reduced. In a future investigation, one would hope that structural integrity could be achieved through digital fabrication as the diversity of materials increases in the marketplace. However, before such improvements in digital fabrication are broadly available in the marketplace, there exists a need to explore the manufacture of comfortable VIPr socket designs through a combination, perhaps, of CAD/CAM and more traditional fabrication techniques. In addition to improvements in fabrication technique, a broader clinical study will be necessary to more deeply understand the relationship between excessive socket pressure and socket variable impedance properties. In the design of transtibial prosthetic sockets, we feel that smoothly varying socket wall impedance in a manner that is inversely proportional to the impedance of the underlying anatomy is of critical importance.

## ACKNOWLEDGMENTS

The authors thank Gerald Berberian and Objet Geometries Inc for allowing the use of the Objet Connex 3D printer. The authors also thank Steve Shannon and Christina Triantafyllou at the McGovern Institute for Brain Research at MIT for assisting with the MRI data collection. Finally, the authors thank David Hill for helping with data processing and prosthetist Bob Emerson for his work in helping them capture the shape of the amputee participant's conventional socket.

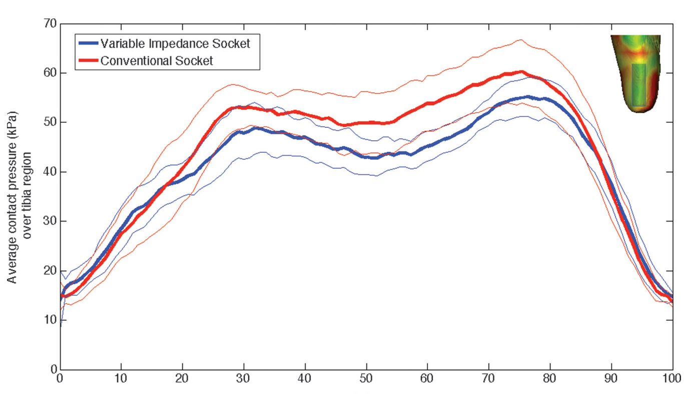


Figure 7. Contact pressures for the variable impedance prosthetic socket and the conventional socket for the same tibia region (shown as the darkened box on the image of the residual limb) are plotted versus percentage stance period. As in Figure 6, shown are mean pressure data ± 1 SD for $n$ = 10 walking gait cycles measured at a preferred gait speed.

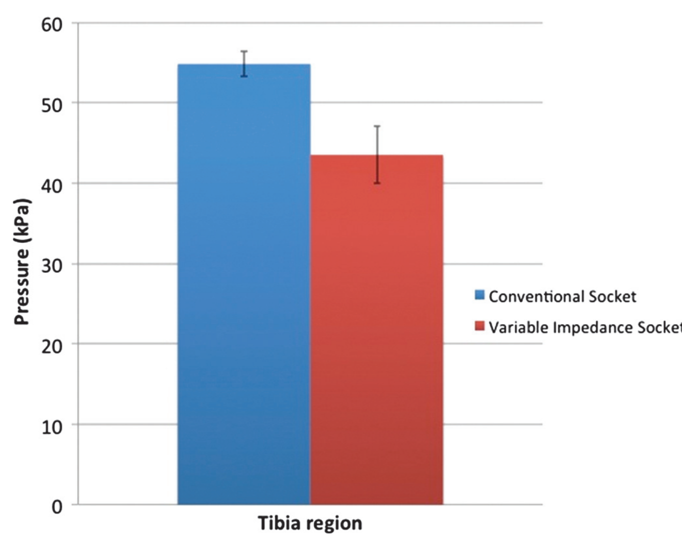


Figure 9. Mean contact pressures ± 1 SD for the two socket interventions measured over the same tibia region during single-leg standing for 4 seconds at 100 Hz.

## REFERENCES


1. Ziegler-Graham K, MacKenzie EJ, Ephraim PL, et al. Estimating the prevalence of limb loss in the United States: 2005 to 2050. *Arch Phys Med Rehabil* 2008;89:422–429.
2. Martinez-Villalpando EC, Herr H. Agonist-antagonist active knee prosthesis: a preliminary study in level-ground walking. *J Rehabil Res Dev* 2009;46:361–373.
3. Au SK, Webber J, Herr H. Powered ankle-foot prosthesis improves walking metabolic economy. *IEEE Trans Robot* 2009;25:51–66.
4. Smith DG, Burgess EM. The use of CAD/CAM technology in prosthetics and orthotics—current clinical models and a view to the future. *J Rehabil Res Dev* 2001;38:327–334.
5. Muller M, Staats TB, Leach M, Fothergill I. Total surface bearing transtibial socket design impression techniques. *J Proc* 2007; available at http://www.oandp.org/publications/jop/2007/2007-49.asp.
6. Faustini MC, Crawford RH, Neptune RR, et al. Design and analysis of orthogonally compliant features for local contact pressure relief in transtibial prostheses. *J Biomech Eng* 2005;127:946–951.
7. Facoetti G, Gabbiadini S, Colombo G, Rizzi C. Knowledge-based system for guided modeling of sockets for lower limb prostheses. *Comput Aided Des Appl* 2010;7:723–737.
8. Moo EK, Osman NAA, Pingguan-Murphy B, et al. Interface pressure profile analysis for patellar tendon-bearing socket and hydrostatic socket. *Acta Bioeng Biomech* 2009;11:37–44.
9. Topper AK, Fernie GR. Computer-aided design and computer-aided manufacturing (CAD/CAM) in prosthetics. *Clin Orthop Relat Res* 1989;256:39–43.
10. Rogers B, Bosker GW, Crawford RH, et al. Advanced trans-tibial socket fabrication using selective laser sintering. *Prosthet Orthot Int* 2007;31:88–100.
11. Torres-Moreno R, Morrison JB, Cooper D, et al. A computer-aided socket design procedure for above-knee prostheses. *Bull Prosthet Res* 1992;29:35–44.
12. Tay FEH, Manna MA, Liu LX. A CASD/CASM method for prosthetic socket fabrication using the FDM technology. *Rapid Prototyping J* 2002;8:258–262.
13. Torres-Moreno R, Saunders CG, Foort J, Morrison JB. Computer-aided and manufacture of above-knee socket. *J Biomed Eng* 1991;13:3–9.
14. Ng P, Lee PVS, Goh JCH. Prosthetic sockets fabrication using rapid prototyping technology. *Rapid Prototyping* 2002;8:53–59.
15. Rogers B, Stephens S, Gitter A, et al. Double-wall, transtibial prosthetic socket fabricated using selective laser sintering: a case study. *J Prosthet Orthot* 2000;12:97–100.
16. Douglas T, Solomonidis S, Sandham W, Spence W. Ultrasound imaging in lower limb prosthetics. *IEEE Trans Neural Rehabil Syst Eng* 2002;10:11–21.
17. He P, Xue KF, Fan Y, Wang YW. Test of a vertical scan mode in 3D imaging of residual limbs using ultrasound. *J Rehabil Res Dev* 1999;36:86–93.
18. Zheng Y, Mak AFT, Lue B. Objective assessment of limb tissue elasticity: development of a manual indentation procedure. *J Rehabil Res Dev* 1999;36:71–85.
19. Buis A, Condon B, Brennan D, et al. Magnetic resonance imaging technology in transtibial socket research: a pilot study. *Gait Posture* 2006;43:883–890.
20. Zhang M, Mak, FT, Chung AIK, Chung KH. MRI investigation of musculoskeletal action of transfemoral residual limb inside a prosthetic socket. 1998 *Proceedings of the 20th Annual International Conference of the IEEE Engineering in Medicine and Biology Society*. 20:2741–2743.
21. Udai AD, Sinha AN. Processing magnetic resonance images for CAD model development of prosthetic limbs socket. 2008*IEEE Region 10 and the Third International Conference on Industrial and Information Systems*. 70:1–5.
22. Novacheck TF. The biomechanics of running. *Gait Posture* 1998; 7:77–95.


.